Atomistic simulation of the behavior of diamond under compressive stress

Y. Uemura
National Institute for Research in Inorganic Materials, 1-1.Namiki, Tsukuba-Shi, Ibaraki 305, Japan
(Received 8 August 1994; revised manuscript received 1 November 1994)

The atomistic model, which simulates the behavior of diamond under uniaxial tension in a [111] direction, has been presented in a previous paper. The model is constructed with a pair-potential method that is based on a tight-binding approximation and a static relaxation process, and has been termed a rigid-tetrahedron model. This model will be applied here to a case of uniaxial compression. A stress-strain relationship can be obtained from the equilibrium condition of the system in small external compression. A cubic polynomial relationship between stress and strain is observed, while the initial curvature of the curve has an opposite sign to the case in tension. A value of the fracture strength of diamond in compression is estimated to be $(1.8\text{–}4.3)\times 10^2$ GPa depending on the boundary condition; it is rather high compared to the value in tension of 0.8×10^2 GPa. The fracture behaviors of diamond in large compression are different from those in tension. It seems that fracture occurs by the formation of a slip plane and the crack propagates via the movement of the edge dislocations appearing at the neighborhood of the crack edges.

The failure strength of diamond in compression is especially important in some practical uses like the pressure anvil cell. Ruoff and his colleagues have done considerable work in evaluating the strengths of covalent crystals in uniaxial loading by using a finite-elasticity method.[1–3] They have computed the compressive and tensile strengths of perfect crystals by using the experimental data of the second- and third-order elastic constants.[4] It is very interesting that the results of our atomic-model calculations are comparable with those of their macroscopic elastic method.

An atomistic model that evaluates the mechanical properties of covalent crystals has been proposed in a previous report.[5] The atomistic model proposed there is rather simple and intuitive. The basic procedures of the model are constructed with a pair-potential method which is based on a tight-binding approximation and a static relaxation process, and was termed a rigid-tetrahedron model in the previous report.[5,6] The fracture behaviors of diamond in tension along the [111] uniaxial direction were discussed there mainly in terms of the effects of vacancies and boundary conditions. It was presented that the crack propagated through the (111) plane perpendicular to the external force direction. We will simulate here the behavior of diamond in compression along the [111] direction, which is realized by providing negative initial strains to a system.

When small strains are initially applied to a diamond crystal, the virtual external stress σ_{111} obtained in a relaxation calculation converges to a certain value σ^*_{111} as the system approaches an equilibrium state. The relationship between initial strain and the corresponding convergent value σ^*_{111} for some equilibrium states is shown in Fig. 1 under two boundary conditions (free and fixed in the x direction). The straight line obtained from the experimental value of the elastic stiffness constant of diamond,[7] $C_{11}=6.7$ eV/Å^3, and the best-fit curves to the calculated points are also shown by solid (curve A) and dotted (curve C) lines, respectively. The results in the best-fit procedure indicate the nonlinear form of the cubic polynomials for the free-boundary condition,

$$\sigma^*_{111}=5.0S(1+2.45S+0.85S^2)\ ,$$

and for the fixed-boundary condition,

$$\sigma^*_{111}=5.1S(1+2.45S+0.68S^2)\ .$$

In the figure, the two curves cannot be resolved and they are denoted as C in the present results. The coefficients of the linear term, 5.0 and 5.1 eV/Å^3, are the same as in the respective cases of tension, while the initial curvatures are positive and contrast with the case of ten-

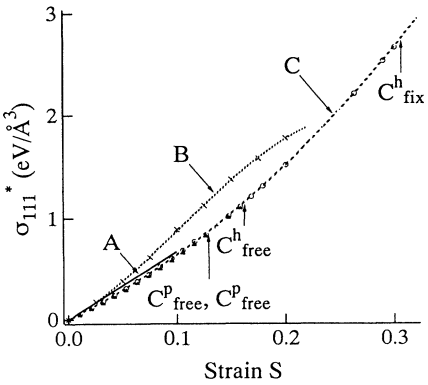

FIG. 1. Relationship between stress and strain; curve A: experimental, curve B: plotted from Ref. 3, and curve C: present results. The two curves for the free- and the fixed-boundary conditions cannot be resolved. $C^p_{free}, C^p_{fix}, C^h_{free}$, and C^h_{fix} represent the critical points in the respective cases. The superscripts p and h denote the point vacancy and the homogeneous crystal, respectively.

sion. For comparison, the [111] uniaxial stress and strain curve which was calculated by finite-elasticity method in Ref. 3 is cited (curve *B*). Though the curvatures have the same sign as each other, initially they show opposite tendencies in the large-strain region.

Crystal systems show fracture behavior when the absolute value of the initial strain is larger than a certain value. The corresponding stress is referred to as the critical strength of the crystal. The value of $C^h_{\rm free}$, which is the critical strength of the perfect diamond crystal in compression mode under the free-boundary condition, is found to be 1.1 eV/Å^3=1.8×10^2 GPa, while the value under the fixed-boundary condition is 2.7 eV/Å^3=4.3×10^2 GPa. The former value is twice the value in tension, but still smaller than the value of Ref. 3. The latter is rather larger than that of Ref. 3 and is comparable with the value reported in Ref. 8. The fixed-boundary condition in the x direction may correspond to the experimental situation of the diamond anvil cell under a uniaxial compressive loading with confining pressure.

As a typical example of fracture by large initial strain, the relationship between the maximum net force $G_{\rm max}$ and the number of iterations is shown in Fig. 2 for a crystal including a point vacancy for $S=-0.137$. The spikes which reflect bond breakage can be seen in the figure. At an early stage of the iterations, an atomic pair whose bond is broken appears in the neighborhood of the vacancy site. With progress in the iteration, the positions of bond breakage seem to extend for the two directions [112] and $[\bar{1}\,\bar{1}\,2]$ in the (111) plane with inclination angle about 20° to the stress direction (the c axis). Edge dislocations with core directions parallel to the y axis are observed in the neighborhoods of both crack edges. The dislocation centers move toward the boundary regions of the z direction with further iterations. They are finally stopped at the neighborhood of the boundary by the fixed-boundary condition in the z direction. The atomic positions and their energies at this stage are shown in Fig. 3(a) and their net force diagram in Fig. 3(b). The arrows in the figures indicate the dislocation positions. The diameter of the circle at each atomic site in Fig. 3(a) denotes roughly the magnitude of the site energy and the maximum circle corresponds to an atom whose energy is larger than the dangling-bond energy. The diameter of each site shown in Fig. 3(b) indicates the instability of the atom position. In Fig. 3(b), unstable atoms exist around the vacancy site rather than in the neighborhood of the dislocation at this stage of the iteration, though the apparent stress concentration seems to occur first at the neighborhood of the dislocations. The fracture behavior under a fixed-boundary condition in the x direction resembles the results of the case under the free-boundary condition, while the progress of bond breakage seems to be slower in this case.

The effects of vacancy clusters on fracture are evaluated. Only paired vacancies are considered here, in the two typical modes as in the case of tension, one a linkage in the [111] direction (longitudinal) and the other in the $[1\bar{1}2]$ direction (transverse).

The fracture behavior of a crystal with a pair of double vacancies in transverse mode is compared to the case of the point vacancy. The critical strain of this case is found to be $S_c=-0.121\pm0.005$, which is smaller than the value for the point vacancy, and this tendency is the same as in the case of tension. On the other hand, for a crystal including pair vacancies in the longitudinal mode, the critical strain and the strength are found to be -0.163 ± 0.005 and 1.8×10^2 GPa, which are higher than the values for a crystal including a point vacancy and the same as those of the perfect crystal under the free-boundary condition. The atomic structures and their energies for the strain $S=-0.179$ and 4000 iterations are shown in Fig. 4. Three crack (111) planes are recognized parallel to each other in the figure, one through the va-

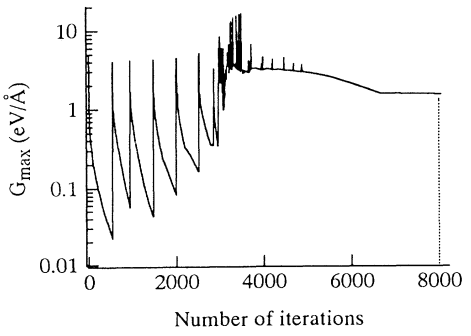

FIG. 2. Maximum net force vs number of iterations for a crystal including a point vacancy under the free-boundary condition. The compressive strain is −0.137.

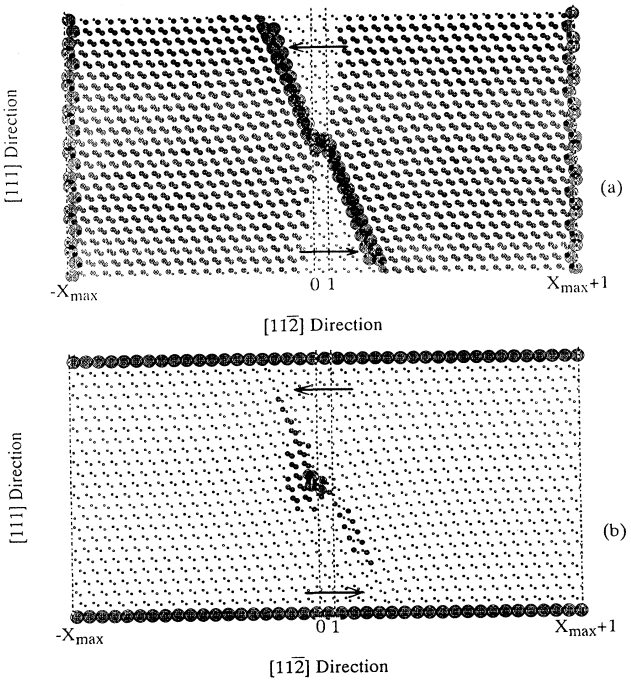

FIG. 3. Atomic structure and energy diagram (a) and force diagram (b) at 8000 iterations.

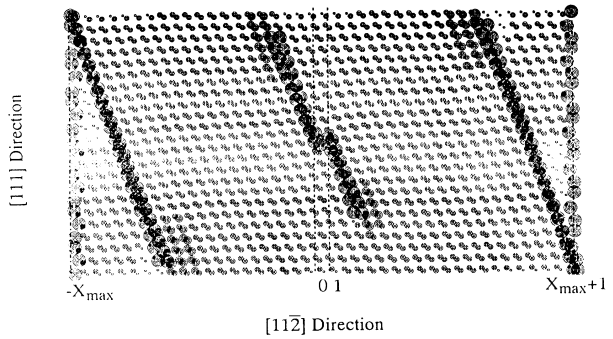

FIG. 4. Atomic structure and energy diagram for a crystal including a pair of vacancies in the longitudinal mode under the free-boundary condition at 3000 iterations for $S=-0.179$.

cancy region and the remaining two terminated at the boundary regions in the x and z directions. The latter two cracks are also observed for the case of the perfect crystal under the free-boundary condition. It is interesting that the crack propagation starts from vacancies and crystal boundaries at the same compression strength.

The failure behavior of the perfect crystal under the fixed-boundary condition in the x direction is rather different from that under the free-boundary condition. With a strain over a critical value in the former case, each atom has one dangling bond initially and the maximum net force decreases abruptly below the tolerance value. The residual stress of the uppermost layer, σ_{111}, converges to the very small value 0.024 eV/Å^3. This might indicate that the perfect diamond crystal is uniformly crushed by larger external compression than the critical one. This critical strength of the perfect crystal seems to be very large compared with that under the free-boundary condition as presented above. Cracks originating at the boundary region do not appear in this case. In the atomic configuration for the longitudinal mode under the fixed-boundary condition only one crack through the vacancy region is observed. The strength is found to be 2.0×10^2 GPa, which is larger than the strength for the longitudinal mode under the free-boundary condition.

We have evaluated the strengths and the fracture behaviors of diamond under a uniaxial external force by the rigid-tetrahedron model. The behaviors in compression are found to be rather different from those in tension. First, the nonlinear relationships between uniaxial stress and strain show contrasting results in the initial curvature for the respective cases, and the tendencies agree with the results from the finite elasticity method.[3]

The effects of the boundary condition which is fixed or free in the x direction can be neglected for the crystal including vacancies. Attention should be paid, however, to the boundary condition for fracture behavior in the cases of the perfect crystal and of the crystal including pair vacancies in the longitudinal mode.

The Poisson ratio, which has not been observed in tension, is obtained in compression but the absolute value is still lower by one order of magnitude than the experimental value. It also depends greatly on the external stress, which was indicated by Ruoff and Luo[9] without a definite functional form. The Poisson ratio is a rather macroscopic quantity and the direct comparison of our result with experiment may be meaningless at present.

In the failure behaviors, shear stress, which has not been observed in tension, seems to play a dominant role in compression. The movement of an edge dislocation seems to induce crack propagation and to construct a slip plane. Because the boundary condition is periodic in the [110] direction, a [110] slip line may be visualized on a (111) surface unless there is a fixed boundary condition in the z direction. This behavior may correspond to the situation of the hexagonal ring cracks on an octahedron face observed by Howes,[10] where the side lines of the hexagon were in the [110] direction on the (111) surface.

The author wishes to thank Dr. Y. Inomata and Dr. Y. Sato at National Institute for Research in Inorganic Materials for helpful discussions of the mechanical properties of materials.

[1]A. L. Ruoff, J. Appl. Phys. **49**, 197 (1978).
[2]D. A. Nelson, Jr. and A. L. Ruoff, J. Appl. Phys. **50**, 2763 (1979).
[3]J. Whitlock and A. L. Ruoff, Scr. Metall. **15**, 525 (1981).
[4]H. J. McSkimin and P. Andreatch, Jr. J. Appl. Phys. **35**, 3312 (1964).
[5]Y. Uemura, Phys. Rev. B **49**, 6528 (1994).
[6]Y. Uemura, Phys. Status Solidi B **167**, 51 (1991).
[7]M. H. Grimsditch and A. K. Ramdas, Phys. Rev. B **11**, 3139 (1975).
[8]A. L. Ruoff, H. Xia, H. Luo, and Y. K. Vohra, Rev. Sci. Instrum. **61**, 3830 (1990).
[9]A. L. Ruoff and H. Luo, J. Appl. Phys. **70**, 2066 (1991).
[10]V. R. Howes, in *The Physical Properties of Diamond,* edited by R. Berman (Clarendon, Oxford, 1965), Chap. 6.